International Journal of Power Electronics and Drive System (IJPEDS)
Vol. 8, No. 4, December 2017, pp. 1932~1942
ISSN: 2088-8694, DOI: 10.11591/ijpeds.v8i4.pp1932-1942

Predictive Control of AC/AC Matrix Converter

Siti Hajar Yusoff[1], Nur Shahida Midi[2], Sheroz Khan[3], Majdee Tohtayong[4]
[1,2,3]Department of Electrical and Computer Engineering, International Islamic University Malaysia, Malaysia
[4]Department of Electrical Engineering, Princess of Naradhiwas University, Thailand

Article Info

Article history:

Received Apr 11, 2017
Revised Sep 26, 2017
Accepted Oct 11, 2017

Keyword:

Matrix converter
Model predictive control
Power supply
Voltage regulation

ABSTRACT

This work investigates the usage of Model Predictive Control (MPC) for a three phase conventional matrix converter with low pass filter at the input and output side. The conventional matrix converter has 3 input and 3 output which gives 27 switching state. From this design, a MPC is incorporate to control the output voltage and the input currents for all the phases. The design of the proposed controller is based on the input current controller and output voltage controller with load observer. The proposed MPC using cost function will select the minimized switching state to be applied to next switching. This gives a sinusoidal output voltages and input currents. A simulation and experimental studies are presented to validate the proposed control scheme.

Corresponding Author:

Siti Hajar Yusoff,
Department of Electrical and Computer Engineering,
Level 3, E1 Block, Faculty of Engineering,
International Islamic University of Malaysia,
Jalan Gombak, 53100, Kuala Lumpur, Malaysia.
Email: sitiyusoff@iium.edu.my

1. INTRODUCTION

In the last few years, considerable research efforts have been dedicated to the development of high performance ac power supplies for many applications such as uninterruptible power supplies (UPS), automatic voltage regulators, programmable ac source, and ground power units for aircraft [1]. A direct AC/AC matrix converter (DMC) “all silicon” structure is preferable over the classical inverter and rectifier that has a dc link. This is due to the lack of bulky dc link electrolytic capacitors or inductors providing a more compact and lighter solution [2]. These advantages together with sinusoidal input currents, bidirectional power flow and a controllable input power factor as well as higher input power quality, have catalyzed industrial attention on matrix converter technology [2], [3]. A number of different modulation strategies have been established for Matrix Converter such as Alesina-Venturini method and space vector modulation (SVM) technique, which have been the subject of various research papers in literature [4-8]. These strategies are then combined with feedback control loops to provide a full regulation of the converter system according to the specific application.

In recent years Model Predictive Control (MPC) has proved to be an interesting alternative for the control of any power electronics applications including matrix converter systems [9-12] also thanks to modern development of high processing power microprocessors. MPC has several advantages such as quick dynamic response, doesn’t required modulator, easy to include non-linearities and constraints of the system and is possible to include other system requirements in the controller [11-13]. The prediction of its future behavior over a time horizon is done using a model of the system. The desired behavior of the system is presented in term of a cost function. MPC is known as an optimization controller due to its nature of selecting the minimized cost function in order to obtain the future desired actuation. Considering the Matrix Converter is a system with finite number of states and has a range of possible combination of switching state, the MPC optimization can be simplified and further reduced to the prediction of the system behavior for each of this state. Then, each prediction in this state is assessed using the cost function and the state that minimizes it, is selected. MPC method has been well presented for multilevel inverter in [13], the current control in a matrix converter in [14], [15], [16], [22] and [23], a three phase inverter in [10] and [17], and an active front end rectifier in [18]. This paper discusses on how MPC scheme can be applied to conventional Matrix Converter with input and output low pass filters. The goal of the control is to deliver high quality output voltage, generating low distortion input currents with unity power factor operation. The controller uses a model of the system to predict, at every sampling time the input reactive power and the output voltage for each possible switching state; then, a cost function is used for selecting the switching state that will be applied in the next sampling time on the base of minimization of reactive power and output voltage error. This is achieved with a single control loop without using a traditional cascaded control structure and provides also regulation of the input current. Additionally, a full load observer is employed to estimate the output currents due to the unknown system linear load. Simulation results obtained in SABER environment, confirm the effectiveness of the proposed solution, that minimizes the control complexity and reduce the number of sensors required for measurements.

2. DIRECT MATRIX CONVERTER MODEL

2.1. Converter Structure

The three-phase conventional Direct Matrix Converter with input and output low pass filters considered in this paper is shown in Figure 1.

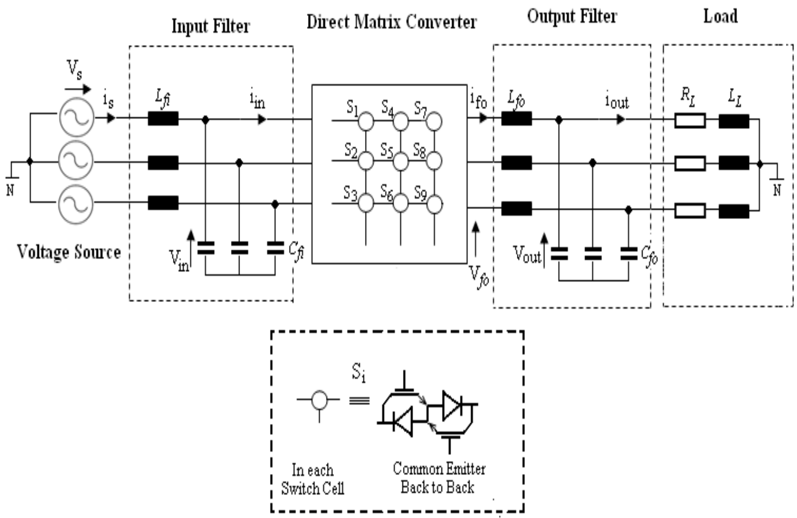

Figure 1. Direct Matrix Converter power supply topology

This Direct Matrix Converter consists of nine bidirectional switches connecting directly a three-phase source to a three-phase load and generating 27 valid switching states [19]. The allowed 27 switching states are generated based on the restriction of the matrix converter topology; the load can't be in an open circuit due to its inductive nature and input phases can't be connected in short circuit. The switching function is defined as:

$$S_i = \begin{cases} 1, & S_i \ closed \\ 0, & S_i \ open \end{cases} \tag{1}$$

Where $i = 1,2 \ldots 9$. Based on (1) and the valid switching states, the converter model can be expressed as follows:

$$\begin{bmatrix} V_{foa} \\ V_{fob} \\ V_{foc} \end{bmatrix} = \begin{bmatrix} S_1 & S_2 & S_3 \\ S_4 & S_5 & S_6 \\ S_7 & S_8 & S_9 \end{bmatrix} \begin{bmatrix} V_{ina} \\ V_{inb} \\ V_{inc} \end{bmatrix} \tag{2}$$

$$\begin{bmatrix} i_{ina} \\ i_{inb} \\ i_{inc} \end{bmatrix} = \begin{bmatrix} S_1 & S_4 & S_7 \\ S_2 & S_5 & S_8 \\ S_3 & S_6 & S_9 \end{bmatrix} \begin{bmatrix} i_{foa} \\ i_{fob} \\ i_{foc} \end{bmatrix} \tag{3}$$

Where $\boldsymbol{V_{fo}}$ and $\boldsymbol{i_{fo}}$ are the output voltage and the output current of the converter whilst $\boldsymbol{V_{in}}$ and $\boldsymbol{i_{in}}$ are the input voltage and the input current of the converter.

The input LC filter connected to the supply is used to filter the high frequency current harmonics while the output LC filter is used to reduce the switching harmonics in the output voltage to improve the output power quality. With reference to Fig. 1 the variables $\boldsymbol{V_s}$, $\boldsymbol{i_s}$, $\boldsymbol{i_{fo}}$, $\boldsymbol{V_{in}}$ and $\boldsymbol{V_{out}}$ are measured while $\boldsymbol{i_{in}}$ and $\boldsymbol{V_{fo}}$can be calculated using Equation (2) and (3); the load current $\boldsymbol{i_{out}}$ is unknown and will be predicted ($\boldsymbol{i^p_{out}}$)using an observer as described in section 3.2C.

2.2. Filters Model

The system model is then completed by adding the influence of input and output filter. The LC input filter continuous model is represented by the following Equations:

$$\boldsymbol{V_s = L_{fi}\frac{di_s}{dt} + i_s R_{fi} + V_{in}} \tag{4}$$

$$\boldsymbol{i_s = i_{in} + C_{fi}\frac{dV_{in}}{dt}} \tag{5}$$

Where, L_{fi} is the input filter inductor, R_{fi} is the input filter resistor and C_{fi} is the input filter capacitor. The output filter continuous model can be described as follows:

$$\boldsymbol{V_{fo} = L_{fo}\frac{di_{fo}}{dt} + i_{fo} R_{fo} + V_{out}} \tag{6}$$

$$\boldsymbol{i_{fo} = i^p_{out} + C_{fo}\frac{dV_{out}}{dt}} \tag{7}$$

Where, L_{fo} is the output filter inductor, R_{fo} is the output filter resistor and C_{fo} is the output filter capacitor

3. MODEL PREDICTIVE CONTROL

In designing this closed loop MPC controller, the following control objectives are defined:

1) Achieve low distortion input currents with unity power factor
2) Achieve high quality control of the output voltage
3) Generate an accurate estimation of the load current

3.1. Control Structure

Figure 2 shows a block diagram of the proposed matrix converter system and predictive control implemented. As it can be seen, the predictive control consists of input and output predictive models, minimization of cost function and state selection.

The input predictive model is based on the discretized system input Equations including the LC filter; it predicts the source current based also on the input current of the matrix converter which depends on the observed load current through the matrix converter. Based on the measured values at sampling instant k this model allows the prediction of the input reactive power at the instant k+1, which will be then used to construct the cost function *g*. The output model is based on the output LC filter, on the observed load current and on the matrix converter output current depending on the input voltage; it is able to predict the output voltage at the instant k+1 to be used in the cost function *g*.

The cost function to be minimized by the MPC includes the output voltage error and the input reactive power error (considering a zero-reference reactive power and the voltage output reference as dictated by the application specifications).

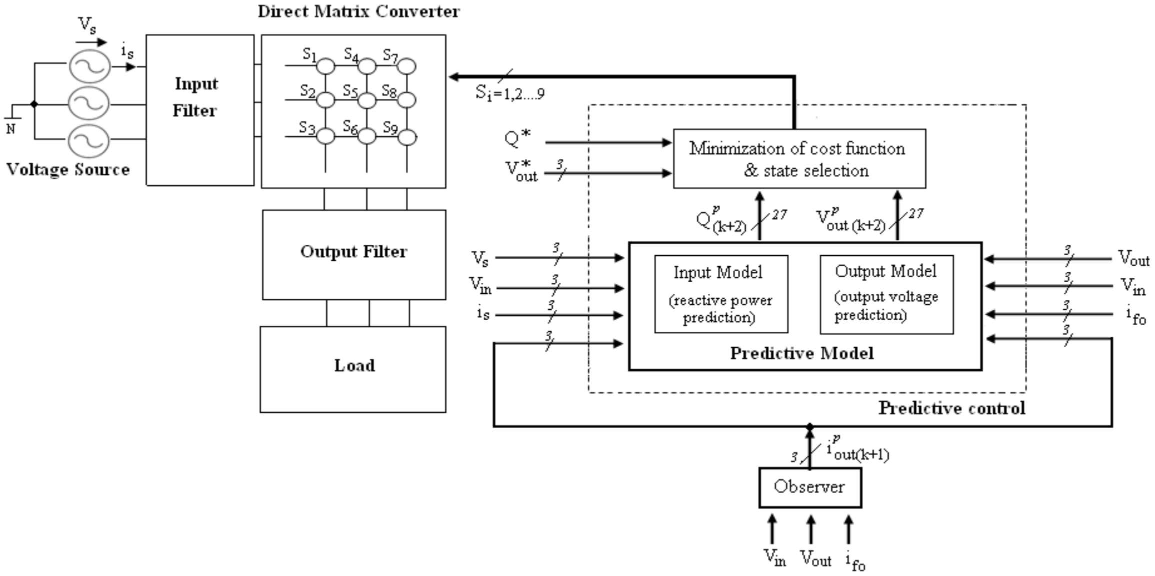

Figure 2. Control scheme of Model Predictive Control

At every sampling time, the output state which produces the smallest value of the cost function g is selected from the 27 possible states. This selected switching state is then applied in the following sampling time (k+2), given the control implementation delay of one sampling period [20]. Detailed description of the prediction models and the cost function g are provided in the following.

3.2. Prediction Models

3.2.1. Input Model

A discrete time model of the input side expressed into a state space form is developed to estimate the next value of the input current assuming the currents and voltages measurements at the k[th] sampling time. Equations (4) and (5) can be rewritten in the form of a continuous state space model as follows

$$\dot{\boldsymbol{x}}(t) = \underbrace{\begin{bmatrix} 0 & {}^{1}/_{C_{fi}} \\ -{}^{1}/_{L_{fi}} & {}^{-R_{fi}}/_{L_{fi}} \end{bmatrix}}_{\boldsymbol{A_{in}}} \boldsymbol{x}(t) + \underbrace{\begin{bmatrix} 0 & -{}^{1}/_{C_{fi}} \\ {}^{1}/_{L_{fi}} & 0 \end{bmatrix}}_{\boldsymbol{B_{in}}} \boldsymbol{u}(t) \tag{8}$$

Where;

$$\boldsymbol{x}(t) = \begin{bmatrix} \boldsymbol{V_{in}}(t) \\ \boldsymbol{i_s}(t) \end{bmatrix} \text{ and } \boldsymbol{u}(t) = \begin{bmatrix} \boldsymbol{V_s}(t) \\ \boldsymbol{i_{in}}(t) \end{bmatrix} \tag{9}$$

A discrete state space model can be derived from (8) using zero order hold method. Considering a sampling period T_s, we obtain:

$$\boldsymbol{x}(k+1) = \boldsymbol{A}\boldsymbol{x}(k) + \boldsymbol{B}\boldsymbol{u}(k) \tag{10}$$

Where;

$$\boldsymbol{A} = e^{\boldsymbol{A_{in}}T_s} \cong \begin{bmatrix} a_1 & a_3 \\ a_2 & a_4 \end{bmatrix} \tag{11}$$

$$\boldsymbol{B} = \int_0^{T_s} e^{\boldsymbol{A_{in}}(T_s-\tau)}\, \boldsymbol{B_{in}} d\tau \cong \begin{bmatrix} b_1 & b_3 \\ b_2 & b_4 \end{bmatrix} \qquad (120$$

Thus, the input current prediction can be easily derived as;

$$\boldsymbol{i_s}(k+1) = a_2\boldsymbol{V_{in}}(k) + a_4\boldsymbol{i_s}(k) + b_2\boldsymbol{V_s}(k) + b_4\boldsymbol{i_{in}}(k) \tag{13}$$

$$\boldsymbol{i_s}(k+2) = a_2\boldsymbol{V_{in}}(k+1) + a_4\boldsymbol{i_s}(k+1) + b_2\boldsymbol{V_s}(k+1) + b_4\boldsymbol{i_{in}}(k+1) \tag{14}$$

The instantaneous reactive input power can be predicted based on the predictions of the input current as shown in Equation (14);

$$Q^p(k+2) = Im\{\boldsymbol{V_s}(k+2)\boldsymbol{\bar{\iota}_s}(k+2)\} \tag{15}$$

$$Q^p(k+2) = V_{s\beta}(k+2)i_{s\alpha}(k+2) - V_{s\alpha}(k+2)i_{s\beta}(k+2) \tag{16}$$

Where $\boldsymbol{\bar{\iota}_s}$ is the complex conjugate of vector $\boldsymbol{i_s}$ whilst the subscripts α and β represent the real and the imaginary components of the associated vector. Line voltages are low frequency signals thus assuming $\boldsymbol{V_s}(k) \approx \boldsymbol{V_s}(k+1) \approx \boldsymbol{V_s}(k+2)$ and $\boldsymbol{V_{in}}(k+1)$ is calculated from (10), such as:

$$\boldsymbol{V_{in}}(k+1) = a_1\boldsymbol{V_{in}}(k) + a_3\boldsymbol{i_s}(k) + b_1\boldsymbol{V_s}(k) + b_3\boldsymbol{i_{in}}(k) \tag{17}$$

$\boldsymbol{i_{in}}(k+1)$ is derived from (3) with one sampling step ahead where $\boldsymbol{i_{fo}}(k+1)$ is based on (25).

3.2.2. Output Model

The continuous system model in Equations (6) and (7) can be rewritten in the state space form as follows:

$$\dot{\boldsymbol{x}}(t) = \underbrace{\begin{bmatrix} {-R_{fo}}/{L_{fo}} & -{1}/{L_{fo}} \\ {1}/{C_{fo}} & 0 \end{bmatrix}}_{\boldsymbol{A_{out}}} \boldsymbol{x}(t) + \underbrace{\begin{bmatrix} {1}/{L_{fo}} & 0 \\ 0 & {-1}/{C_{fo}} \end{bmatrix}}_{\boldsymbol{B_{out}}} \boldsymbol{u}(t) \tag{18}$$

Where;

$$\boldsymbol{x}(t) = \begin{bmatrix} \boldsymbol{i_{fo}}(t) \\ \boldsymbol{V_{out}}(t) \end{bmatrix} \text{ and } \boldsymbol{u}(t) = \begin{bmatrix} \boldsymbol{V_{fo}}(t) \\ \boldsymbol{i^p_{out}}(t) \end{bmatrix} \tag{19}$$

Considering a sampling period T_s, the state space model in (18) can be discretized:

$$\boldsymbol{x}(k+1) = \boldsymbol{Ax}(k) + \boldsymbol{Bu}(k) \tag{20}$$

Where;

$$\boldsymbol{A} = e^{\boldsymbol{A_{out}}T_s} \cong \begin{bmatrix} a_5 & a_7 \\ a_6 & a_8 \end{bmatrix} \tag{21}$$

$$\boldsymbol{A} = e^{\boldsymbol{A_{out}}T_s} \cong \begin{bmatrix} a_5 & a_7 \\ a_6 & a_8 \end{bmatrix} \tag{22}$$

Thus, the output voltage prediction can be easily derived as followed;

$$\boldsymbol{V^p_{out}}(k+1) = a_8\boldsymbol{V_{out}}(k) + a_6\boldsymbol{i_{fo}}(k) + b_6\boldsymbol{V_{fo}}(k) + b_8\boldsymbol{i^p_{out}}(k) \tag{23}$$

$$\boldsymbol{V^p_{out}}(k+2) = a_8\boldsymbol{V^p_{out}}(k+1) + a_6\boldsymbol{i_{fo}}(k+1) + b_6\boldsymbol{V_{fo}}(k+1) + b_8\boldsymbol{i^p_{out}}(k+1) \tag{24}$$

$\boldsymbol{i_{fo}}(k+1)$ is calculated from (20), such as:

$$\boldsymbol{i_{fo}}(k+1) = a_5\boldsymbol{i_{fo}}(k) + a_7\boldsymbol{V_{out}}(k) + b_5\boldsymbol{V_{fo}}(k) + b_7\boldsymbol{i^p_{out}}(k) \tag{25}$$

$\boldsymbol{V_{fo}}(k+1)$ is derived through $\boldsymbol{V_{in}}(k+1)$ in (17) based on relation in (3). Whereas $\boldsymbol{i^p_{out}}(k+1)$ is obtained from the observer (33), as described in the next section.

3.2.3. Load Current Observer

The unknown load current $\boldsymbol{i_{out}}$ can be estimated using a full order state observer. Assuming the load current dynamics slower enough compared to the system sampling frequency, the load current can be approximated as a constant during one sampling period, in which:

$$\frac{di_{out}}{dt} = 0 \tag{26}$$

Taking Equation (26) into the filter model, the discrete state space filter model can be written as in (27);

$$\dot{\boldsymbol{x}}(t) = \underbrace{\begin{bmatrix} {-R_{fo}}/{L_{fo}} & {-1}/{L_{fo}} & 0 \\ {1}/{C_{fo}} & 0 & {-1}/{C_{fo}} \\ 0 & 0 & 0 \end{bmatrix}}_{\boldsymbol{A_{ob}}} \boldsymbol{x}(t) + \underbrace{\begin{bmatrix} {1}/{L_{fo}} \\ 0 \\ 0 \end{bmatrix}}_{\boldsymbol{B_{ob}}} \boldsymbol{u}(t) \tag{27}$$

Where;

$$\boldsymbol{x}(t) = \begin{bmatrix} \boldsymbol{i_{fo}}(t) \\ \boldsymbol{V_{out}}(t) \\ \boldsymbol{i_{out}}(t) \end{bmatrix} \text{ and } \boldsymbol{u}(t) = [\boldsymbol{V_{fo}}(t)] \tag{28}$$

Based on (27), there are two measurable variables: the filter current $\boldsymbol{i_{fo}}$ and the output voltage $\boldsymbol{V_{out}}$. The output of this system is therefore defined as follows;

$$\boldsymbol{y}(t) = \underbrace{\begin{bmatrix} 1 & 0 & 0 \\ 0 & 1 & 0 \end{bmatrix}}_{\boldsymbol{C_{ob}}} \boldsymbol{x}(t) \tag{29}$$

The full state observer is used to estimate the state vector $\boldsymbol{x}$ thus its Equation is defined as:

$$\frac{d\hat{\boldsymbol{x}}(t)}{dt} = \boldsymbol{A_{ob}}\hat{\boldsymbol{x}}(t) + \boldsymbol{B_{ob}}\boldsymbol{u}(t) + \boldsymbol{L}(\boldsymbol{y}(t) - \boldsymbol{C_{ob}}\hat{\boldsymbol{x}}(t)) \tag{30}$$

where **L** is the observer gains matrix. This matrix **L** will define the observer dynamics. In this design, the observer gain is chosen so the observer poles produce a dynamic several times faster than the open loop system dynamics. Equation (30) can be further written as:

$$\frac{d\hat{\boldsymbol{x}}(t)}{dt} = [\boldsymbol{A_{ob}} - \boldsymbol{L}\boldsymbol{C_{ob}}]\hat{\boldsymbol{x}} + [\boldsymbol{B_{ob}} \quad \boldsymbol{L}] \begin{bmatrix} \boldsymbol{V_{fo}} \\ \boldsymbol{i_{fo}} \\ \boldsymbol{V_{out}} \end{bmatrix} \tag{31}$$

Therefore, the observer output is the estimated load current $\boldsymbol{i^{p}_{out}}$ based on measurements of the output voltage $\boldsymbol{V_{out}}$, the input voltage $\boldsymbol{V_{in}}$ needed to obtain $\boldsymbol{V_{fo}}$ through (2), and the filter current $\boldsymbol{i_{fo}}$.

Considering a sampling period T_s, the state space model in (31) can be discretized:

$$\begin{bmatrix} i_{fo}(k+1) \\ V_{out}(k+1) \\ i_{out}(k+1) \end{bmatrix} = \begin{bmatrix} A_{o1} & A_{o2} & A_{o3} \\ A_{o4} & A_{o5} & A_{o6} \\ A_{o7} & A_{o8} & A_{o9} \end{bmatrix} \begin{bmatrix} i_{fo}(k) \\ V_{out}(k) \\ i_{out}(k) \end{bmatrix} + \begin{bmatrix} B_{o1} & B_{o2} & B_{o3} \\ B_{o4} & B_{o5} & B_{o6} \\ B_{o7} & B_{o8} & B_{o9} \end{bmatrix} \begin{bmatrix} V_{fo}(k) \\ i_{fo}(k) \\ V_{out}(k) \end{bmatrix} \tag{32}$$

Thus $\boldsymbol{i^{p}_{out}}(k+1)$ is defined as follows;

$$\boldsymbol{i^{p}_{out}}(k+1) = (A_{o7} + B_{o8})\boldsymbol{i_{fo}}(k) + (A_{o8} + B_{o9})\boldsymbol{V_{out}}(k) + A_{o9}\boldsymbol{i_{out}}(k) + B_{o7}\boldsymbol{V_{fo}}(k) \tag{33}$$

3.2.4. Cost Function

The block diagram of the proposed control scheme is shown in Figure 2. The measured variables $\boldsymbol{V_s}$, $\boldsymbol{i_s}$, $\boldsymbol{i_{fo}}$, $\boldsymbol{V_{in}}$ and $\boldsymbol{V_{out}}$ and the estimated load current $\boldsymbol{i^p_{out}}$ are feed into the predictive model which is then used to calculate the predictions $\boldsymbol{V^p_{out}}(k+2)$ and $\boldsymbol{Q^p}(k+2)$ as in (16) and (24).

As stated earlier, the control objectives are to produce a regulated and sinusoidal output voltage and to generate a low harmonic distortion input current together with unity input power factor operation. The input side objectives can be achieved by minimizing the predicted reactive power given in Equation (16) considering a zero reference as shown in (35).

$$\Delta Q[k+2] = |Q^*[k+2] - Q^p[k+2]| \tag{34}$$

Where;

$$Q^*[k+2] = 0 \tag{35}$$

Thus Equation (34) is rewritten as;

$$\Delta Q[k+2] = |Q^p[k+2]| \tag{36}$$

The output side objective can be achieved by minimizing the error between the output voltage reference $\boldsymbol{V^*_{out}}(k+2)$ and the respective predicted value $\boldsymbol{V^p_{out}}(k+2)$ as follows;

$$\Delta V_{out}[k+2] = V^*_{out}[k+2] - V^p_{out}[k+2] \tag{37}$$

The resulting cost function g that includes both objectives, is obtained by adding (36) and (37). Thus;

$$g(k+2) = \lambda|Q^p[k+2]| + \Delta V_{out}[k+2] \tag{38}$$

Where λ is a weighting factor. The weighting factor is selected based on the THD of the input and output current as presented in [9]. Further techniques of selecting the weighting factors are described in [21] and can eventually be used. A value of g=0 gives perfect output voltage tracking and unity power factor at the input side. This cost function g is evaluated for every possible switching state: the state among $S_{1\ldots27}(k+2)$ that minimizes g is selected and applied at the Direct Matrix Converter output in the k+2 sampling period.

4. SIMULATION AND EXPERIMENTAL RESULTS

In order to analyse the effectiveness of the proposed method, the predictive control strategy and the observer algorithm are simulated. Using the full schematic model of the system, all simulations are done under balanced three phase supply voltages and balanced three phase RL load. It has to be noticed that in the simulations, the application of the next switching state is instantaneous, so no delay compensation is used throughout the modelling.

Input and output fundamental frequency is chosen at 50 Hz and the output voltage is controlled at 42V. Figure 3 shows the simulation results for source current and voltage in one input phase. It is possible to notice that unity power factor and quasi sinusoidal source currents are obtained. The input current is sinusoidal and in phase with the supply voltage, which confirm the control of the input power factor (PF) is achieved. Figure 4 shows the spectrum analysis of the input phase current.

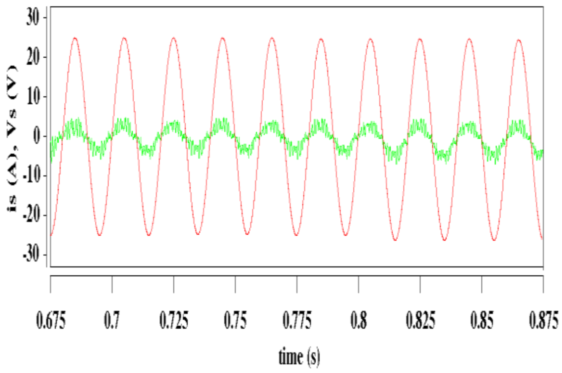

Figure 3. Input current and voltage ($V_s/2$) during steady state operation with reactive power minimization

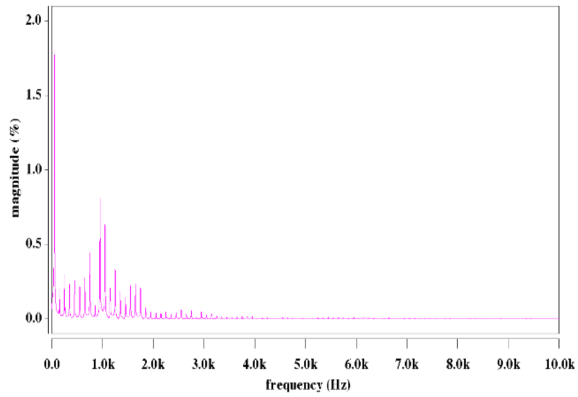

Figure 4. Harmonic spectra of input current 80µs (T_s), THD=8%

Figure 5 shows a voltage step change in amplitude of the reference voltage (V_o^*) from 20V to 42V. As expected, the output voltage (V_o) has a good tracking and following the reference voltage (V_o^*).

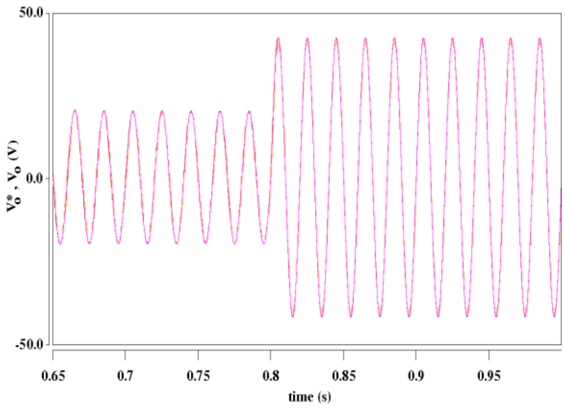

Figure 5. A step-in output reference voltage

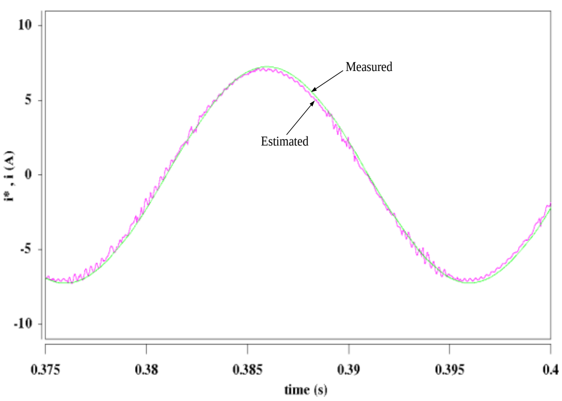

Figure 6. Observer load current estimation and the measured load current

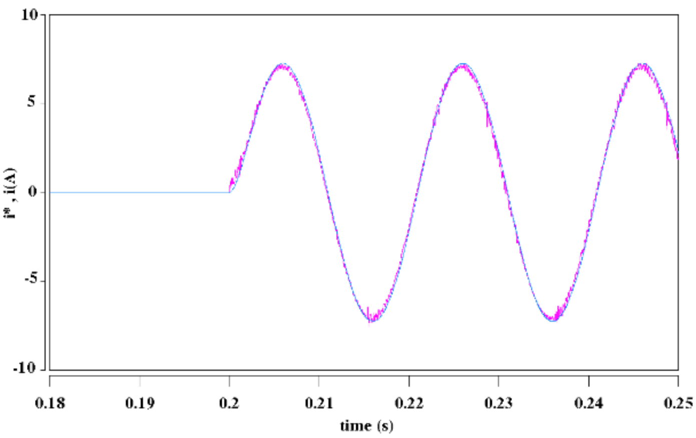

Figure 1. Measured and estimated output current for resistive-inductive load step

Figure 6 illustrates the estimated observer load current compared to the measured load current during steady state. The result demonstrating the excellent observer tracking capabilities, with good estimation and fast dynamic response. Whilst, the measured load current and the estimated load current for a load step is applied to one phase of the load is shown in Figure 7 for linear load. This load step is applied at time 0.2s. The estimated load current gives a good response in a quick load change condition. It concludes that the observer loads current estimation show fast dynamic response during this transient event.

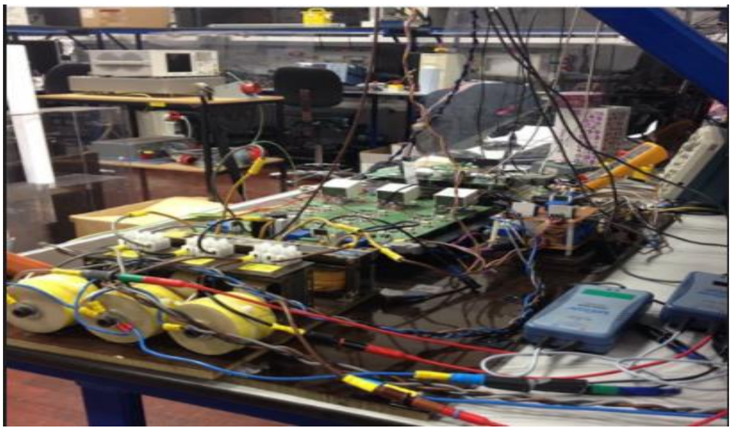

Figure 8. Experimental setup of a Direct AC/AC Matrix Converter

Experimental setup of this work is shown in Figure 8 above. Results for a step change in voltage amplitude reference (V_o^*) from 20V to 42V is shown in Figure 9. It can be seen that the output voltage (V_o) exhibits good dynamic tracking even with sudden reference change. Figure 9(a) shows the output voltage phase *a* during a reference step change at time -0.020s whilst Figure 9(b) shows all three phases of the output voltages *a*,*b* and *c* during a reference step change at time -0.020s.

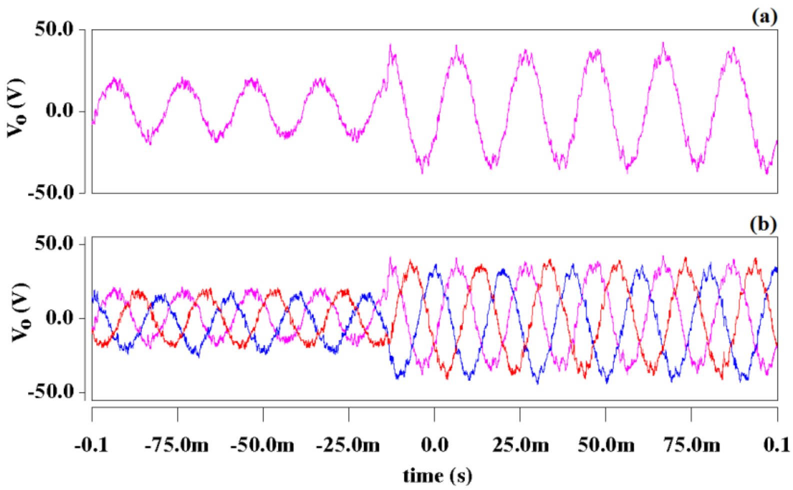

Figure 9. A step-in output reference voltage for output phase using both output voltage and input current based MPC

5. CONCLUSION

This paper shows a direct optimal control method for a matrix converter based power supply system, where a multiple control target (input reactive power minimization and output voltage regulation) is achieved with the implementation of a single control loop and without the need for modulator. The control scheme is simple, it is easy to implement and can achieve excellent steady state performance and a fast-dynamic response, as confirmed by simulation results showing unity input power factor operation and sinusoidal output voltage with low harmonic distortion. The implementation of full load current observer has provided a precise estimation of the unknown load current and with good tracking performance.

ACKNOWLEDGEMENTS

This work is supported by Ministry of Higher Education Malaysia (Kementerian Pendidikan Tinggi) under Research Initiative Grant Scheme (RIGS) number RIGS15-150-0150.

REFERENCES

[1] Katsis, D.W., P.W.; Clare, J.C.; Empringham, L.; Bland, M., *"A utility power supply based on a four-output leg matrix converter,"* Industry Applications Conference, 2005. Fourtieth IAS Annual Meeting. Conference Record of the 2005, 2-6 Oct. 2005. 4: p. 2355- 2359

[2] Wheeler, P.W.R., J.; Clare, J.C.; Empringham, L.; Weinstein, A., "Matrix converters: a technology review. Industrial Electronics," *IEEE Transactions* on 2002 49(2): p. 276 - 288

[3] Wheeler, P.W., Clare, J.C., Empringham, L., Bland, M., Kerris, K.G, Matrix converters. EEE Ind. Appl. Mag, 2004. 10: p. 59– 65.

[4] Tuusa, M.J.a.H., "Comparison of simple control strategies of space-vector modulated indirect matrix converter under distorted supply voltage," *IEEE Trans. Power Electron*, Jan.2007. 22(1): p. 139–148.

[5] P. Nielsen, F.B., and J. K. Pedersen, *"Space vector modulated matrix converter with minimized number of switching and feedforward compensation of input voltage unbalance,"* Proc. Power Electron. Drives and Energy Syst. (PEDES'96), New Delhi, India, Jan. 8–11. 2: p. 833–839.

[6] D. Casadei, G.S., A. Tani, and L. Zarri, "Matrix converter modulation strategies: A new general approach based on space-vector representation of the switch state," *IEEE Trans. Ind. Electron*, Apr. 2002. 49(2): p. 370–381.

[7] Sul, Y.D.Y.a.S.K., "Carrier-based modulation technique for matrix converter," *IEEE Trans. Power Electron*, Nov. 2006. 21(6): p. 1691–1703.

[8] M. Lee, P.W., and C. Klumpner, "Space vector modulated multilevel matrix converters," *IEEE Trans. Ind. Electron*, Oct. 2010. 57(10): p. 3385–3394.

[9] S. Kouro, P.C., R. Vargas, U. Ammann, and J. Rodriguez, "Model Predictive Control - A Simple and Powerful Method to Control Power Converters," *IEEE Trans. on Industrial Electronics*, June 2009. 56(6): p. 1826-1838.

[10] J. Rodriguez, J.P., C. Silva, P. Correa, P. Lezana, and P. Cortes, "Predictive Current Control of a Voltage Source Inverter," *IEEE Trans. on Industrial Electronics*, Feb 2007. 54(1): p. 495-503.

[11] P. Cortes, M.P.K., R. M. Kennel, D. E. Quevedo, and J. Rodriguez, "Predictive Control in Power Electronics and Drives," *IEEE Trans. on Industrial Electronics*, Dec. 2008. 55(12): p. 4312-4324.

[12] P. Zanchetta, J.C., P. Wheeler, D. Katsis, M. Bland, L. Empringham, "Control Design of a Three-Phase Matrix Converter AC Power Supply Using Genetic Algorithms," *IEEE Transaction on Industrial Electronics*, January 2008. 55(1): p. 209 - 217.

[13] Cortes, P.O., G. ; Yuz, J.I. ; Rodriguez, J. ; Vazquez, S. ; Franquelo, L.G., "Model Predictive Control of an Inverter With Output LC Filter for UPS Applications," *Industrial Electronics, IEEE Transactions*, June 2009 56(6): p. 1875 - 1883

[14] Corté ; s, P.W., A. ; Kouro, S. ; Rodriguez, J. ; Abu-Rub, H. ;, "Model Predictive Control of Multilevel Cascaded H-Bridge Inverters," *Industrial Electronics, IEEE Transactions*, Aug. 2010 57(8): p. 2691 - 2699

[15] R. Vargas, J.R., U. Ammann, and P. W. Wheeler, "Predictive current control of an induction machine fed by a matrix converter with reactive power control," *IEEE Trans. Ind. Electron*., Dec. 2008. 55(12): p. 4362–4371.

[16] Rivera, M.R., C. ; Rodrí ; guez, J. ; Wheeler, P. ; Bin Wu ; Espinoza, J.R. ;, "Predictive Current Control With Input Filter Resonance Mitigation for a Direct Matrix Converter," *Power Electronics, IEEE Transactions*, Oct. 2011. 26(10): p. 2794 - 2803

[17] S. Muller, U.A., and S. Rees, "New time-discrete modulation scheme for matrix converters," *IEEE Trans. Ind. Electron*, Dec. 2005. 52(6): p. 1607–1615.

[18] J. Rodríguez, J.P., C. Silva, M. Salgado, S. Rees, U. Ammann,P. Lezana, R. Huerta, and P. Cortés, "Predictive control of a three-phase inverter," *Electron. Lett*, Apr. 29, 2004. 40(9): p. 561–562.

[19] Quevedo, D.A., R. ; Perez, M. ; Cortes, P. ; Lizana, R., "Model Predictive Control of an AFE Rectifier with Dynamic References," *Power Electronics, IEEE Transactions*, 13 December 2011(99): p. 1.

[20] P. Zanchetta, P.W., L. Empringham, J. Clare, *"A Three-Phase Utility Power Supply Based on the Matrix Converter,"* Proceedings of IET_EPA, March 2009. 2(2): p. 156-162.
[21] Cortes, P.K., S. ; La Rocca, B. ; Vargas, R. ; Rodriguez, J. ; Leon, J.I. ; Vazquez, S. ; Franquelo, L.G., *"Guidelines for weighting factors design in Model Predictive Control of power converters and drives,"* Industrial Technology, 2009. ICIT 2009. IEEE International Conference, 10-13 Feb. 2009: p. 1 - 7
[22] Yusoff, S., et al. *"Predictive Control of a direct AC/AC matrix converter power supply under non-linear load conditions,"* in 2012 15th International Power Electronics and Motion Control Conference (EPE/PEMC). 2012.
[23] Yusoff, S., et al. *"Predictive control of a direct AC/AC matrix converter for power supply applications,"* in 6th IET International Conference on Power Electronics, Machines and Drives (PEMD 2012). 2012.

BIOGRAPHIES OF AUTHORS

Siti Hajar Yusoff obtained her Ph.D. in Electrical and Electronic Engineering from University of Nottingham. Her research interest is mainly in the Power Electronics, Control system, and Electrical Drives. She is currently an Assistant Professor of Department of Electrical and Computer Engineering, Faculty of Engineering, International Islamic University of Malaysia (IIUM).

Nur Shahida Midi obtained her Doctor of Engineering (Science and Technology) from Tokai University, Japan. Her research interests are mainly high voltage engineering and electrical power engineering. She is currently an Assistant Professor of Department of Electrical and Computer Engineering, Faculty of Engineering, International Islamic University of Malaysia (IIUM).

Sheroz Khan received his B.Sc in Electrical Engineering from the NWFP University of Engineering and Technology (NWFP UET), Peshawar, Pakistan, in 1982. He got M.Sc in Microelectronic & Computer Engineering at Surrey University, UK. He completed his PhD to re-join his parent university in 1994. Since 2000, he has been working within the department of ECE at the IIUM Kuala Lumpur. He is heading Wireless Communication and Signal Processing Research Group. He is the Curriculum Advisory Committee chair and member since 2006. He is the Senior Member of the IEEE and Chartered Engineer (UK). He has remained Chair of the IEEE Malaysia Chapter for 2012 while working as a secretary of the IEEE IMS Malaysia Chapter for 2013-2016. He is the founder of the International Conference on Intelligent Systems Engineering (ICISE), and International Conference on Smart Instrumentation, Measurement and Application (ICSIMA). Currently he is working on ICISE2018 jointly organized by KoE of IIUM asnd FET of IIU Islamabad, Pakistan to be held on the Gombak Campus of IIUM here in Kuala Lumpur Malaysia in March 20-21, 2018. This is as part of the IIUM-IIU Islamabad link program, Sheroz Khan is coordinator of. Sheroz Khan is also the coordinator of the link program of IIUM and University of Limoges (France), which has been functioning well since 2014 with undergraduate students exchnages and IIUM PhD Researchers placement at Xlim, Limoges.

Majdee Tohtayong was born in Pattani, Thailand, in 1981. He completed his bachelor in power electronics from King Mongkut's University of Technology North Bangkok (KMUTNB), Bangkok, Thailand, in 2005, and the masters degree in electrical engineering from Prince of Songkla University (PSU), Hatyai campus, Thailand, in 2008, and works as a lecturer at Department of Electrical Engineering, Princess of Naradhiwas University (PNU), Narathiwat, Thailand. He is currently pursuing a Ph.D. degree in Engineering at department of electrical and computer engineering (ECE), international islamic university malaysia (IIUM), Malaysia. His current research interests include Power converter topology, PWM strategies, Modular multilevel converters, large scale of power converter circuit, interleaved power converters, harmonic reduction, Modeling and simulation of power electronics system, Wireless power transfer system, Contactless power transfer, and HVDC.